

## DEVELOPMENT OF A LOW EMITTANCE DC GUN FOR SMITH-PURCELL BWO FEL

K. Kasamsook<sup>#</sup>, K. Akiyama, K. Nanbu, M. Kawai, F. Hinode, T. Muto, T. Tanaka, M. Yasuda, Y. Mori, H. Hama, Laboratory of Nuclear Science, Tohoku University, 1-2-1 Mikamine, Taihaku-ku, Sendai 982-0826, Japan

### Abstract

An electron DC gun capable for producing very low emittance beam is now under evaluation of beam qualities at Laboratory of Nuclear Science, Tohoku University. The DC gun employs a high voltage of 50 kV to extract electrons, which is suitable to drive Smith-Purcell backward wave oscillator free electron laser (BWO FEL) [1]. From a result of numerical simulation using a 3-D finite difference time domain (FDTD) method [2], the BWO FEL oscillation at the terahertz wavelength region maybe achieved by using the electron beam with an emittance lower than  $1 \pi$  mm mrad. Average power is expected to be more than  $100 \text{ W/mm}^2$ .

In addition to which a very small cathode of  $\text{LaB}_6$  single crystal is employed for the gun [3], the geometrical structure is optimized to produce the lower emittance beam. A numerical calculation of the electro-static model for the DC gun to solve equilibrated beam envelope predicts a normalized beam emittance of  $0.3 \pi$  mm mrad will be possible for the beam current of a couple of hundreds mA. Particularly by applying additional bias voltage between the cathode and the wehnelt, the transverse distribution of electrons is possibly becoming to be an ideal Kapchinskij-Vladimirskij (K-V) beam [4], so that the space charge effect will be minimized.

## INTRODUCTION

### Smith-Purcell BWO FEL

In order to understand the characteristics of the BWO FEL and the interaction between the DC beam and the evanescent waves supported by a grating, an FDTD simulation has been performed. Nonlinear behavior of the Smith-Purcell radiation was already observed [5]. That was coherent and has been presumed to result from the beam microbunching effect due to interaction with the evanescent modes.

We have chosen a model grating for the simulation as indicated in Fig. 1. The period length  $\lambda_g = 400 \mu\text{m}$ , the groove width  $W = 200 \mu\text{m}$ , the groove depth  $d = 300 \mu\text{m}$  and the grating full width  $L = 2 \text{ mm}$ , the number of period of 50 are employed, respectively. The sheet DC beam, which has the emittance of  $1 \pi$  mm mrad for the both directions, is generated by very low horizontal and vertical beta functions of 6.25 cm and 0.4 mm, respectively. Since the evanescent wave is exponentially decreasing as the distance from the grating surface increases, the sheet beam has to travel just above the surface in order to have sufficient overlapping with the evanescent wave (here we have chosen  $100 \mu\text{m}$ ).

FEL Technology I

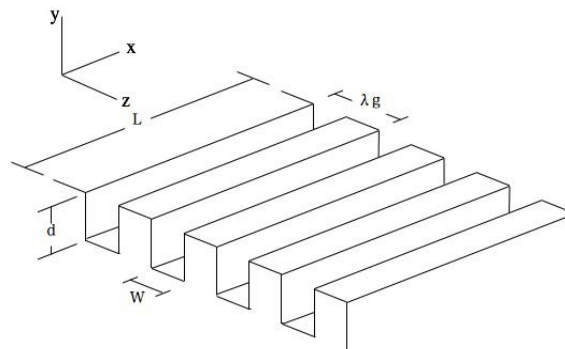


Figure 1: A model grating for FDTD simulations.

The Smith-Purcell BWO FEL is not driven by ponderomotive potential as conventional FELs with wigglers. The microbunching is occurred by the longitudinal electric field ( $E_z$ ) in the evanescent wave, and the conventional Smith-Purcell radiation becomes coherent. The evanescent mode is much more excited by the bunched beam, so that the gain is yielded.

The FDTD simulation was performed with a DC beam current of 150 mA. To avoid beam brow-up the strong external longitudinal field ( $B_z \sim 1 \text{ T}$ ) applied. From the dispersion relation of the evanescent wave [6], the group velocity at the beam frequency negative, so that this is the backward-wave. Time dependent evolutions of radiated power observed at the grating upstream end are shown for two different emittance cases in Fig. 2.

We notice that for the normalized emittance of  $1 \pi$  mm mrad case, the power increased up to several hundreds  $\text{W/mm}^2$  and a damping oscillation was excited after saturation. Meanwhile a larger normalized emittance case, such as  $5 \pi$  mm mrad shown in Fig. 2(b), the FEL oscillation was not occurred. The results show the beam emittance is very crucial for the Smith-Purcell BWO FEL.

The frequency spectrum obtained Fourier transform of the power evolution of Fig. 2(a) is shown in Fig. 3. In this grating case, an intense sub-Terahertz radiation may be obtained.

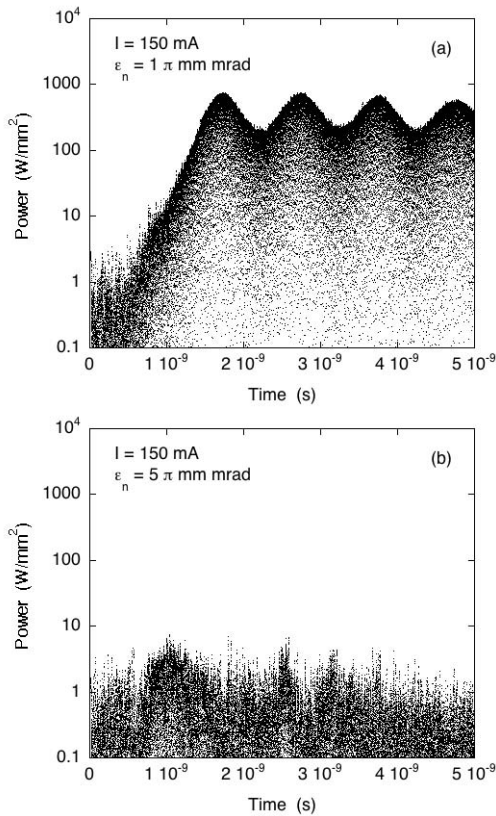


Figure 2: Simulation results of the FDTD Smith-Purcell BWO FEL. (a) The normalized beam emittances are  $1 \pi$  mm mrad, and (b)  $5 \pi$  mm mrad, respectively.

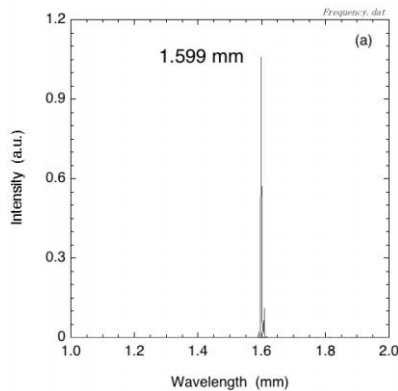


Figure 3: Frequency spectrum of simulated Smith-Purcell BWO FEL (corresponds to Fig. 2(a)).

### Low emittance DC gun

The DC gun has been designed with a wehnelt electrode to manipulate electric field around the cathode. The feasibility study of the gun for the Smith-Purcell BWO FEL has been investigated by the simulation. From the simulation results, we have presumed that the emittance is very sensitive to the equi-potential surface around the cathode. Consequently we found that the equi-

potential surface can be manipulated by applying the negative bias between the cathode and the wehnelt electrode. In the simulation, an extremely low emittance less than  $1 \pi$  mm mrad is achieved [7].

The schematic diagram of DC gun power supply is shown in Fig. 4. The fabrication of the DC gun had been finished and we succeeded to extract the electron beam over 300 mA exceeding our target value [8]. The main design parameters are shown in Table 1. This low emittance DC gun has been studied both experimentally and theoretically. The paper will present the status of the development of the low emittance DC gun.

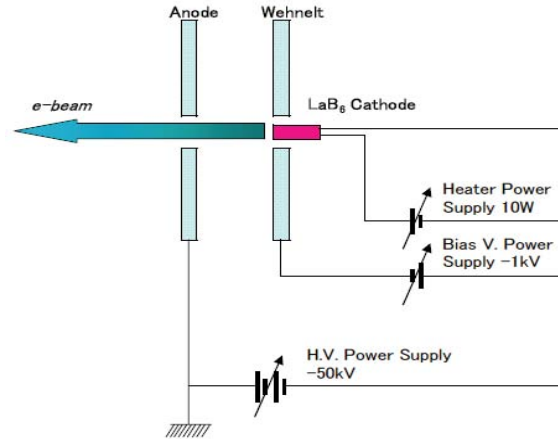


Figure 4: The schematic diagram of DC gun power supply.

Table 1: Design parameters of electron gun.

Beam energy	50 keV (Max.)
Peak current	>300 mA
Pulse width (FWHM)	1-5 $\mu$ sec
Repetition rate	50 pps
Normalized emittance	< $1 \pi$ mm mrad.
Normalized thermal emittance	0.25 $\pi$ mm mrad* *theoretical
Cathode diameter	1.75 mm.

## DC GUN DEVELOPMENT

### Beam quality measurements

An experimental set-up for beam size measurements is depicted in Fig. 5. The beam size was measured at downstream of the DC gun by applying the focusing power of the solenoid lens. The main components in this section are solenoid lens, current transformer (CT), the slit and a Faraday plate. The overall beam current was measured by the CT located at the downstream of the solenoid lens. Meanwhile the beam current passing through the slit was measured by the Faraday plate.

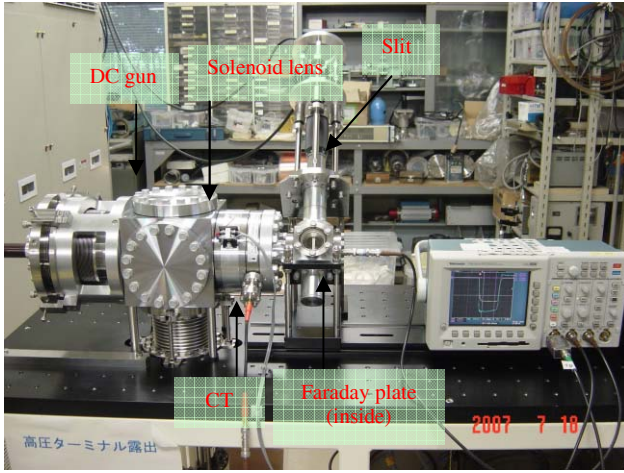


Figure 5: The DC gun configuration for beam size measurement

A slit plate used for the beam size measurement is made of SUS 316L and its thickness is a 50  $\mu\text{m}$ . Two perpendicular slits for X and Y direction with width of  $50 \pm 2 \mu\text{m}$  were manufactured by wire cut method, and its width was measured by a high precision microscope. The moving direction of the slit stage is 45-degree between X and Y axes, because only one move can make two axes scans.

The slit plate was mounted on an insertable and rotatable actuator powered by 5-phase stepping motor (Oriental Motor PK545AW-P7.2). This allowed us to align the slits to the beam and insure the proper angle with respect to the beam. Combining the ball bearing spindle (1 mm pitch for one revolution) and the precise stepping motor, the maximum resolution of step is 1/3600 mm. The scanning speed is around 15 second for one beam profile.

The measurement are made as follow; (1)set the slit movable stage to the initial position at first, then using a Faraday plate get the signal of the beam passing through the slit, (2)go to the next stage position, then repeat again until the end position coming. Signals from the CT and the Faraday plate are connected to digital oscilloscope and analyzed by software.

All measurements were performed at various beam currents of 50, 180 and 430 mA that are corresponding to heater current of 7, 7.5 and 8.0 A, respectively. Taking look at the V-I characteristic curve of our DC gun [8], we have chosen 8 A of heater current for an ordinal operating condition. The minimum rms beam size less than 2 mm in both X and Y directions was obtained at the operating condition. The measured beam profiles are shown in Fig. 6. One can notice the shift of a beam position in each case. Possible reasons are alignment errors of the cathode and the solenoid lens. The beam size becomes bigger when the beam current increases and a stronger focusing strength of the solenoid lens is required to confine the beam. It seems the space charge effects play a significant role for the beam size at the higher beam current.

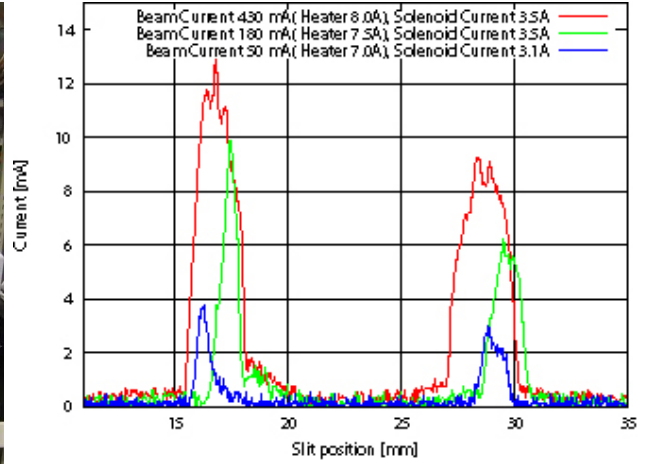


Figure 6: Measured minimum beam size profile at various beam currents.

### Transverse beam emittance

In the following analysis, we assume an axis-symmetric electron beam confined by a longitudinal magnetic field of solenoid lens. This method is used to deduce a tentative beam emittance of our DC gun. So the measurement can be understood by examining the evolution of the rms beam size in a drift length following a thin lens of focal length  $f$ . The beam is transported through a solenoid. In this case, the beam matrix transforms at the slit position given by

$$\sigma^1 = R\sigma^0 R^T, \quad (1)$$

where  $R$  is the transfer matrix in drift space ( $L$ ) and solenoid lens (the magnetic strength,  $Q$ ) represented by

$$R = \begin{pmatrix} 1 & L \\ 0 & 1 \end{pmatrix} \begin{pmatrix} 1 & 0 \\ -Q & 1 \end{pmatrix} = \begin{pmatrix} 1-QL & L \\ -Q & 1 \end{pmatrix}. \quad (2)$$

In this linear analysis, we have explicitly ignored space-charge effect. By applying initial conditions to eq. (1), we can solve the equation for the square of the rms beam size in the term of focal length of the solenoid lens as

$$\sigma_{11}^1 = \langle x_1^2 \rangle = L^2 \sigma_{11}^0 Q^2 - 2[L\sigma_{11}^0 + L^2 \sigma_{12}^0]Q + L^2 \sigma_{22}^0 + 2L\sigma_{12}^0 + \sigma_{11}^0. \quad (3)$$

In this form, we can see that the square of the rms beam size at the end of the drift should depend on the square of the magnetic strength of the solenoid lens. The scan is done by varying the strength of the solenoid lens and measure the beam size at the fixed distance from the lens. In the eq. (3) we can simplify the form as

$$\begin{aligned} \sigma_{11}^1 = \langle x_1^2 \rangle &= aQ^2 + bQ + c = a \left( Q + \frac{b}{2a} \right)^2 + \frac{4ac - b^2}{4a} \\ &= a'(Q + b')^2 + c'. \end{aligned} \quad (4)$$

The normalized rms emittance is calculated by an equation

$$\varepsilon_{n,rms} = \beta\gamma \sqrt{\langle x_0^2 \rangle - \langle x_0 \rangle^2 - \langle x_0 x'_0 \rangle^2} = \frac{\beta\gamma}{2L^2} \sqrt{4a'c'}, \quad (5)$$

where  $\beta$  is the beam velocity divided by light velocity,  $\gamma$  is the relativistic mass factor, and  $a'$ ,  $b'$ ,  $c'$  are coefficients of quadratic function deduced from curve fitting. For solving this problem numerically, an internal MATLAB solver is used [9]. The MATLAB consists of a constrained non-linear least-square fit algorithm based on the Levenberg-Marquardt method. The robustness of the algorithm needs to be assured. Particularly, this algorithm should work for noisy data, such as experimental data.

For the data at the beam current of 430 mA, the emittance is then calculated by fitting the data using the quadratic beam transport equation. The results of fitting are shown in Fig. 7 and Fig. 8. The normalized rms emittances, 2.46 and 2.66  $\pi$  mm mrad are obtained for the horizontal and the vertical axes, respectively

We calculated the propagation of error by eq. (6). The deduced errors are  $\pm 0.89$  and  $\pm 1.05$   $\pi$  mm mrad for the horizontal and vertical normalized rms emittances, respectively.

$$\Delta\varepsilon_{n,rms} = \frac{\beta\gamma}{2L^2} \sqrt{\left(\frac{c'}{a'}\right)\Delta a'^2 + \left(\frac{a'}{c'}\right)\Delta c'^2}. \quad (6)$$

The same analysis was performed on data taken at 50 and 180 mA of beam currents, respectively. The fits to the data give the normalized rms emittance of  $1.14 \pm 1.17\pi$  mm mrad (horizontal emittance) and  $0.82 \pm 0.72$   $\pi$  mm mrad (vertical emittance) for 50 mA. For the beam current of 180 mA, the results are  $1.84 \pm 1.87$  and  $1.72 \pm 1.36$   $\pi$  mm mrad for the horizontal and the vertical normalized rms emittance, respectively. Though these errors seem to be high compared with expected values of normalized rms emittance, anyhow, it seems the current dependence of the emittance exists.

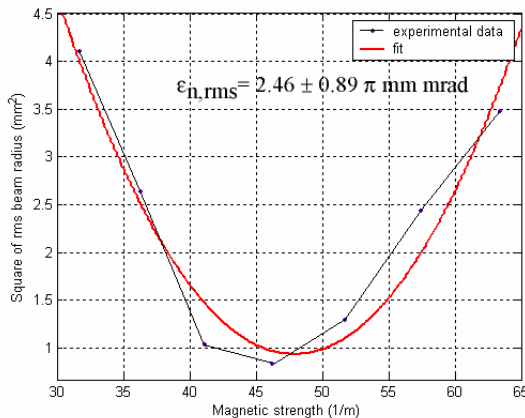


Figure 7: Square of beam radius in the horizontal axis plotted as a function of magnetic strength of solenoid lens.

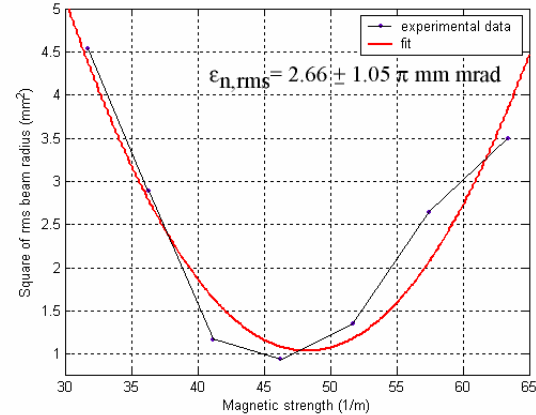


Figure 8: Square of beam radius in the vertical axis plotted as a function of magnetic strength of solenoid lens.

In this linear analysis, we ignore the space charge effects and approximate the effect of solenoid lens by thin lens as well. A rigorous error analysis was not performed in the analysis of the data. We have estimated only the errors result from the uncertainty of the quadratic fit. For this reason, it is highly desired to use the high precision technique instead of the solenoid scanning method to confirm the emittance value.

## SUMMARY

We have developed a very low emittance DC gun employing a single crystal of LaB<sub>6</sub> cathode. Preliminary value of the measured normalized emittance was around 2  $\pi$  mm mrad. Further investigation including manipulation of the equi-potential surface around the cathode by applying the additional bias voltage will be performed.

## REFERENCES

- [1] V. Kumar and K-J. Kim, Phys. Rev E 73 (2006) 026501.
- [2] H. Hama, et al., to be published.
- [3] H. Kobayashi et al., Proc. 1992 Linear Accelerator Conf., Ottawa, Canada, August 1992.
- [4] I.M. Kapchinskij and V.V. Vladimirskij, Proc. Int. Conf. on High Energy Accelerators p. 274 (CERN, GENEVA, 1959).
- [5] J. Urata, M. Goldstein, M.F. Kimmitt, A. Naumov, C. Platt and J. Walsh, Phys. Rev. Lett. 80 (1998) 516
- [6] H. L. Andrews et al., Phys. Rev ST Accel. Beam 8, (2005) 050703.
- [7] K. Kasamsook et al., Proc. FEL2006, Berlin, Germany (2006) 680.
- [8] K. Kasamsook et al., will be appeared in Proc of APAC2007, Indore, India (2007).
- [9] MATLAB, User's Manual, <http://www.mathworks.com/access/helpdesk/help/toolbox/curvefit/curvefit.shtml>